



## Efficient RMS Delay Spread-Based Physical Layer Abstraction Modelling for Enhanced 5G New Radio Performance Evaluation

Bzhar R. Othman<sup>1\*</sup>, Thuraya M. Alqaradaghi<sup>2</sup>, Araz S. Ameen<sup>3</sup>

<sup>1</sup> Communication Engineering Department, Technical College of Engineering, Sulaimani Polytechnic University, Sulaymaniyah, Kurdistan, Iraq

E-mail: [bzhar.rahman@spu.edu.iq](mailto:bzhar.rahman@spu.edu.iq)

<sup>2</sup> Electrical Engineering Department, College of Engineering, Salahaddin University-Erbil, Erbil, Kurdistan, Iraq

<sup>3</sup> Electrical Engineering Department, College of Engineering, University of Sulaimani, Sulaymaniyah, Kurdistan, Iraq

Received: Mar 14, 2024

Revised: May 10, 2024

Accepted: May 19, 2024

Available online: Sep 15, 2024

**Abstract**— Nowadays, Fifth Generation-New Radio (5G-NR) is an important research area in telecommunication field. System level studies are essential to evaluate the performance of wireless systems and signaling techniques prior to practical deployment as well as to research purposes. System level studies of wireless systems involve many links between the base station and the user equipment, many modulations and coding schemes and many operation scenarios. Performing system level studies using detailed physical layer simulation using Link Level Simulator (LLS) is impractical and time consuming. Instead, physical layer abstraction models of wireless systems are used in system level studies. Therefore, this paper proposes a physical layer abstraction model for the 5G-NR cellular system following the Effective Signal to Interference plus Noise Ratio (ESINR) approach. The proposed abstraction model uses a novel Exponential ESINR Mapping (EESM) that involves two tunable parameters to model the Physical Downlink Shared Channel (PDSCH) of the 5G-NR system. The proposed model is validated against detailed LLS of the PDSCH. Novel equations are proposed to model the optimum values of the two tunable parameters of the EESM as a function of the RMS delay spread of the wireless channel for different modulation and coding schemes. The obtained results show that the performance - obtained using the proposed EESM abstraction model - is very close to the performance obtained from the detailed LLS. The run time of the abstraction model is independent of the size of the transport block data size. The abstraction model is 10 times faster than the detailed LLS for a transport block size of 3.1 kbits. This factor increases to 153 when the transport block size is increased to 57.376 kbits. The proposed equations for the EESM and its optimum two tunable parameters can be used as an accurate tool to evaluate the Block Error Rate (BER) and the throughput performance of PDSCH in NR wireless system for different environments.

**Keywords**— Physical layer abstraction; Abstract engine; 5G-new radio; System level study; Performance evaluation.

### 1. INTRODUCTION

The evolution of wireless communication technologies has paved the way for unprecedented advancements, catalysing a connected world poised for the Fifth Generation (5G) wireless technology revolution [1]. As the demand for ubiquitous connectivity burgeons across diverse domains such as industrial automation, smart cities, and immersive multimedia experiences, 5G emerges as a transformative force in enabling ultra-reliable, low-latency communication systems [2, 3].

New Radio (NR) is the radio access technology specified by Third Generation Partnership Project (3GPP) for 5G mobile networks. It is designed to provide enhanced capabilities and

support various use cases, including Enhanced Mobile Broadband (eMBB), Ultra-Reliable Low-Latency Communication (URLLC), and Massive Machine-Type Communication (mMTC) [4]. NR employs advanced techniques such as massive MIMO, beamforming, and flexible spectrum usage across diverse frequency bands to deliver high data rates, low latency, and increased reliability for diverse applications [5].

The connectivity and the service provision between the Base Station (BS) and the User Equipment (UE) in the NR Radio Access Network (RAN) are achieved through layered architecture. The physical layer is the first layer in the protocol stack hierarchy and provides data transport services to/from the upper layers. It is responsible for transmitting raw binary data (0s and 1s) over the wireless medium. It handles the modulation of signals, channel coding, and other processes essential for transmitting information between devices [6]. Specifically in the context of 5G NR, the physical layer involves advanced technologies and methodologies tailored to support the high-speed, low-latency, and diverse use cases characteristic of 5G networks [7]. The main features of 5G NR physical layer includes Low-Density Parity Check (LDPC) channel coding, higher order modulation techniques, Orthogonal Frequency Division Multiplexing (OFDM), flexible frame structures by means of various numerologies, and support for wide channel bandwidth operations at millimetre-wave frequency band [8, 9].

The performance of wireless network can be evaluated using Link-Level Simulator (LLS) and System-Level Simulator (SLS). In the first, a comprehensive and extremely computational model of the physical layer processing of the air interface including channel coding-decoding, multi-antenna processing, and OFDM modulation is used to run the simulations. In the latter, network-based analysis is the focus, with examples of this being resource allocation, mobility, and interference analysis [10]. The LLS is more accurate, but it becomes unfeasible for system level studies that includes many BS-UE links, different Modulation and Coding Scheme (MCS) modes, different antenna configurations, and different operation scenarios. This is due to the huge volume of data processing required at physical layer. Therefore, the SLS is vital for studying the system performance of wireless networks and technologies [11, 12] where the physical layer is typically abstracted to computational efficient algorithms and mathematical models to speed up the simulations.

The physical layer abstraction process for OFDM based system, such as the 5G NR, consist of two primary procedures. Firstly, a parameter called Effective Signal power to Interference plus Noise power Ratio (ESINR) is derived from the values of Signal power to Interference plus Noise power Ratio (SINR) for each subcarrier that can be reported from the channel model. Secondly, the Bit Error Rate (BER), BLER, or the achieved data rate is computed using predefined lookup tables based on the obtained ESINR in the first stage [10].

There are several studies for abstraction modelling of the physical layer for wireless systems such as Long-Term Evolution (LTE) in [13], Wireless Fidelity (Wi-Fi) in [13, 14], and the 5G NR in [10, 15-17]. Also, various techniques, such as Exponential ESINR Mapping (EESM) and Received Bit Mutual Information Rate (RBIR), are used for calculating ESINR depending on the mapping function. The study in [10] used EESM technique and [15] proposed an EESM with the help of machine learning technique. A comparison study between RBIR and EESM is performed in [13, 14, 16] and enhancements is proposed in the name of eRBIR in [14], and eEESM in [13, 17].

The previous mentioned studies are made for only a specific scenario of physical layer parameters. This means that the designed model in these literatures can be used only for a case

of performed study. Also, the effect of a channel model characteristics is not investigated in previous studies. Therefore, this paper proposes a new abstraction model for the 5G NR system using a new EESM formula. The main objectives of the work can be summarised as follows:

- Develop and perform link level simulation for the Physical Downlink Shared Channel (PDSCH) of the 5G NR signalling techniques according to the 3GPP in [8, 9]. This link level simulation is used to create a lookup table for the mapping function between the SINR and BLER of the abstraction model for different MCS modes based [18].
- Propose a novel EESM formula for the abstraction model for the 5G NR PDSCH. The novel EESM formula includes two tunable parameters  $\alpha$  and  $\beta$  in order to improve the accuracy of the abstraction model. Optimum values of  $\alpha$  and  $\beta$  are selected to provide minimum root mean square error (RMS) between the SNR and the ESINR.
- Propose novel equations that models  $\alpha$  and  $\beta$  as function of the RMS delay spread of the wireless channel for different MCS modes in order to improve the availability of the abstract engine.

## 2. SYSTEM MODEL

This section presents the system model of the PDSCH of the 5G NR system. As shown in Fig. 1, the LLS is used to evaluate the BLER performance of the 5G NR PDSCH as a function of the Signal power to Noise power Ratio (SNR) under Additive White Gaussian Noise (AWGN) channel only. Then the SINR of the UE is determined from the fading channel and used to determine the ESINR. The ESINR is then used to estimate the BLER based on the BLER-SNR lookup table. Section 2.1 describes general processing and the LLS of the PDSCH. Section 2.2 presents the proposed abstraction model of the PDSCH for the 5G NR.

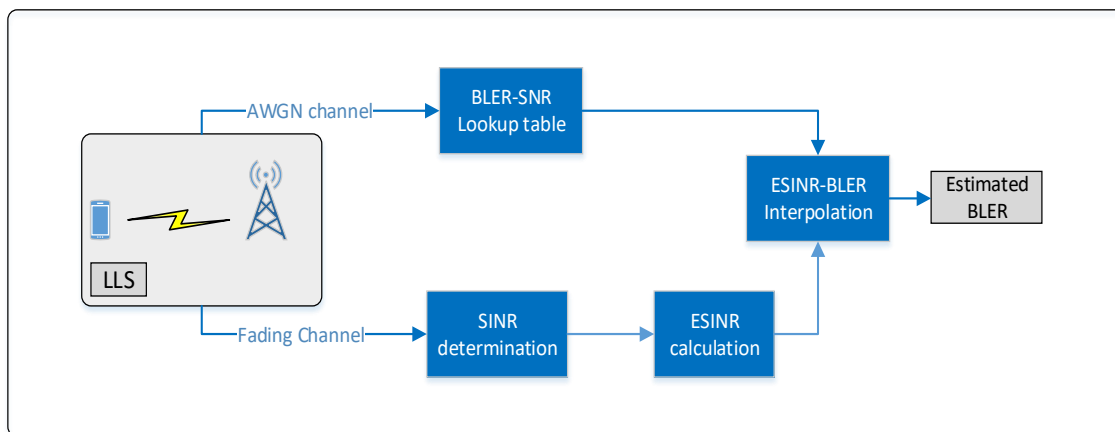


Fig. 1. Schematic diagram of the proposed physical layer abstraction model.

### 2.1. Link Level Simulator

As mentioned earlier, to model the PDSCH of the 5G NR using abstraction model, a link level simulation is required to derive a lookup table for the BLER performance versus SNR. This sub section describes and presents the system model and parameters of the LLS of the 5G NR PDSCH.

Fig. 2 shows the general block diagram of 5G NR PDSCH [19] and Table 1 lists the physical layer parameters of the 5G NR system according to 3GPP Release 16 standards in [6, 9, 20, 21]. The channel encoding process of the data plane uses LDPC code, and the channel

decoding process uses normalized min-sum with 6 decoding iterations. The modulation schemes are M-ary Quadrature Amplitude Modulation (MQAM), with M values of 4, 16, 64, and 256. As presented in Table 2, the number of selected MCS modes are 13 selected based on [18]. The OFDM transmitter uses a system bandwidth of 10 MHz bandwidth composed of 52 resource block [20] and 12 subcarriers per resource block with a subcarrier spacing of 15 kHz [9]. In time axis of the resource grid, the number of symbols per each slot time is 14 symbols [9]. The communication channel between the BS and the UE is modelled using Tapped Delay Line (TDL) type A (TDL-A) that is proposed by the 3GPP for LLS of the 5G NR for Non-Line-of-Sight (NLOS) scenario.

Fig. 3 shows achievable data rate of the selected MCS modes versus SNR obtained from the LLS of the PDSCH of the NR system for a BS-UE link with AWGN channel. It is obvious from the figure that the achievable data rates depend on the received SNR at the user location and the selected MCS mode. Also, the selected MCS mode in this study provides a uniform distribution of the achievable data rate from the minimum to the maximum values [18]. Therefore, the selected set of the MCS modes in the proposed abstract model (see Table 2) can be used to model all the MSC modes of standard 5G-NR standard.

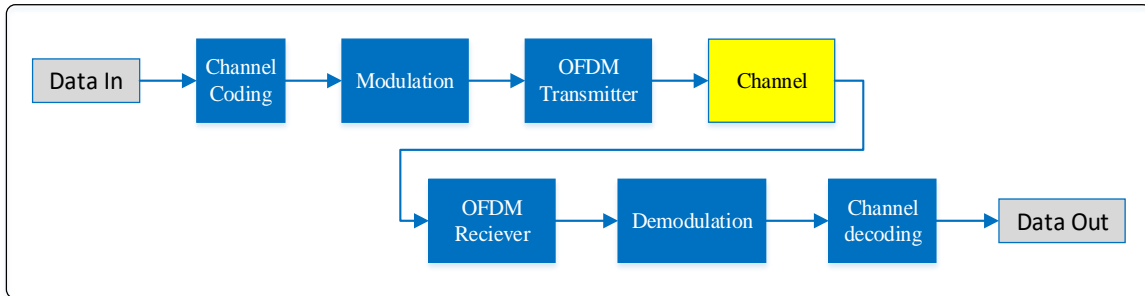


Fig. 2. Basic block diagram of 5G NR PDSCH.

Table 1. Simulated system parameters settings.

Parameter		Value
Channel coding	Type	LDPC
	Decoding Algorithm	Normalized min-sum
	Decoding iteration number	6
Modulation schemes		4QAM, 16QAM, 64QAM, 256QAM
System bandwidth		10 MHz
Subcarrier spacing		15 kHz
OFDM parameters	Number of resource Blocks	52
	Number of subcarriers per resource block	12
	Number of active subcarriers	624
	Number of OFDM symbols per timeslot	14
	Channel Model	AWGN, TDL-A

Table 2. Modulation order and channel coding code rate of the utilized MCS modes.

MCS mode	1	2	3	4	5	6	7	8	9	10	11	12	13
Modulation order	2	2	2	4	4	4	4	4	6	6	8	8	8
Code rate	1/5	1/3	1/2	1/3	1/2	3/5	3/4	8/9	4/5	8/9	1/2	4/5	8/9
Peak data rate [Mbps]	3.1	4.86	7.68	9.73	15.6	19.5	24.6	28.7	38.9	43	31.2	52.2	57.4

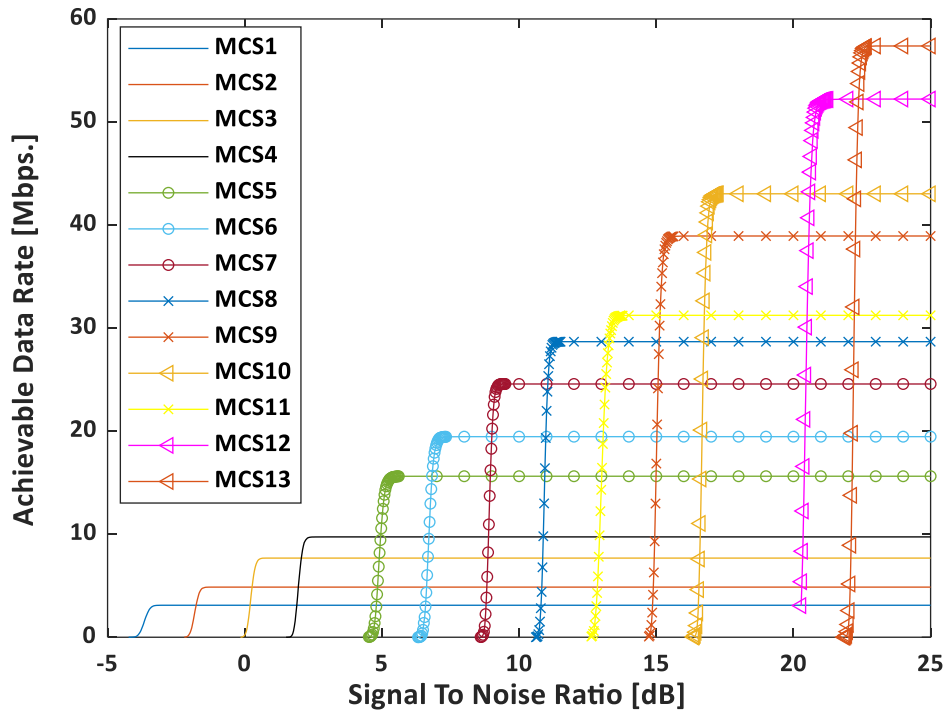


Fig. 3. Achievable data rate for different MCS modes.

## 2.2. Proposed Exponential ESINR Mapping

The abstraction models usually predict the performance of the physical layer as a function of the received SINR. The received SINR is then used to estimate the BLER and/or the achieved data-rate for a given MCS mode. A various received SINR may be observed for each subcarrier in multi-carrier wideband systems. These different SINR values are compressed into a single value called ESINR. Therefore, to estimate the performance of these systems, ESINR mapping is essential. The ESINR summarizes the effect of all SINRs such that the system performance at a given ESINR is equivalent to the performance under (AWGN) channel conditions [10]. This requires a look-up table for performance evaluation or link adaptation under various fading conditions. The steps of modelling the physical layer abstraction for every MCS mode can be summarised as follow:

- Step 1.** Obtain BLER versus SNR using the LLS under AWGN channel condition to create BLER-SNR lookup table.
- Step 2.** Obtain the BLER versus SNR using LLS under AWGN and frequency selective channel condition.
- Step 3.** Calculate the ESINR for each SNR point in Step 2 from the SINR values of the  $N$  subcarriers using Eq. (1). The ESINR is a single value that represent the effective SINR over  $N$  subcarriers.
- Step 4.** Map the ESINR to the BLER of the physical layer using the BLER-SNR lookup table obtained in Step 1.
- Step 5.** Compare the estimated performance in Step 4 with the LLS performance in Step 2.

The calculation and mapping of the ESINR are vital parts of the abstraction physical model since it determines the accuracy of the abstract engine. Therefore, this paper proposes a novel Exponential ESINR Mapping (EESM) for the abstract engine of the 5G NR as defined in

Eq. (1). The ESINR in dB is function of the number of the subcarriers,  $N$ , the SINR of each subcarrier in dB, and the mapping function parameters  $\alpha$  and  $\beta$ .

$$ESINR = -\beta \ln\left(\frac{1}{N} \sum_{n=1}^N e^{-SINR}\right) + \alpha \quad (1)$$

In EESM, given an experimental BLER measured in a fading channel for a specific MCS mode, the values of  $\alpha$  and  $\beta$  are calibrated such that the ESINR of that channel approximates the SNR that would produce the same BLER, with the same MCS, in AWGN channel conditions. As expressed in Eq. (2), the value of  $\alpha$  and  $\beta$  are adjusted to find the optimal values such that the Mean Square Error (MSE) between the ESINR and SNR for all simulated BLER points is minimum.

$$\beta, \alpha = \arg \min_{\beta, \alpha} |SNR_{AWGN} - ESINR(\beta, \alpha)|^2 \quad (2)$$

### 3. VALIDATION OF THE PROPOSED EESM MODEL

In this section, the proposed EESM physical layer abstraction technique is validated against results from the LLS of the NR PDSCH. The LLS for the PDSCH of the 5G NR in Fig. 2 is developed using MATLAB software based on parameters from Table 1. As illustrated in Fig. 1, the LLS is first used to evaluate the BLER versus SNR performance under AWGN channel condition only. The obtained BLER versus SNR performance serves as lookup table to be used in the abstract model. Second, the LLS is used to determine the BLER versus SINR performance of the PDSCH at the same SNR values considering AWGN and frequency selective channel with RMS DS of 30 ns. The frequency selective channel is generated using TDL-A channel model. Third, the proposed equation, Eq. (1), is used to calculate the ESINR for every SINR (SNR) point. Finally, the abstract engine is used to estimate the BLER performance of the system using the calculated ESINR under the same channel realization. A comparison of the results of the physical simulator and abstraction model is performed to optimize the mapping function parameters  $\alpha$  and  $\beta$ .

In system level studies, it is vital for the abstraction model to provide the desired performance metric as accurate as the physical layer simulator at the same SNR value with AWGN channel utilization in an ideal case. This implies that the difference between the SNR and the ESINR to be minimized as expressed in Eq. (2). In a shade of this principle, the Root Mean Square Error (RMSE), is used as an evaluation metric. All simulated BLER points between 1 and  $10^{-3}$  are considered to calculate RMSE using Eq. (3):

$$RMSE = \sqrt{\frac{1}{P} \sum_{i=1}^P (SNR_{AWGN}(i) - ESINR(i))^2} \quad (3)$$

In Eq. (3), both  $SNR_{AWGN}$  and  $ESINR$  are in dB at the  $i^{\text{th}}$  BLER sample, and  $P$  is a total number of samples.

Fig. 4 shows the BLER simulation result with respect to the SNR and ESINR for different MCS modes. The solid line graphs in Fig. 4 represents the BLER versus SNR obtained from the LLS of PDSCH NR under AWGN channel condition. The star marked plots represent the BLER of a fading channel condition versus ESINR that are obtained using the proposed EESM model. The figure shows a best match between of BLER performances of both models for different MCS modes. The figure shows that ESINR and AWGN-SNR are approximately the same for the same BLER. Therefore, the ESINR can be interpolated with look up table to predict BLER. This means that the proposed EESM abstract engine performs accurately and can be used as an accurate SLS tool alternative to the LLS of the PDSCH for the NR in system level studies. The optimized

values of ESINR function parameters ( $\alpha$  and  $\beta$ ) are determined as the values that make the RMSE of Eq. (3) minimum value.

The grid search optimization method is used with a step of 0.01 and 0.001 to determine the optimum values of  $\alpha$  and  $\beta$ , respectively. The process is started with the values that make RMSE greater than 0.1 as the maximum acceptable RMSE value. Fig. 5 illustrates an example of how the optimized values are determined for MCS 2 according to the proposed RMSE metric. In this example, the minimum RMSE is 0.029 and occurs at the trail 22. Therefore, the optimum values of  $\alpha$  and  $\beta$  for MCS 2 are -1.63 and 0.031, respectively. The same procedure is applied for the other MCS modes.

Table 3 lists the optimized values of  $\alpha$  and  $\beta$  for different MCS modes used in this study. Comparing the RMSE values of the proposed model in Eq. (1) with the results from the literature studies, a significant improvement can be observed in the accuracy in our proposed model. The RMSE values in the proposed model for MCS modes 3, 5, and 6 are 0.038, 0.041, and 0.037 respectively, while RMSE values for the same MCS modes reported in [16] are 0.07, 0.08, 0.13 respectively.

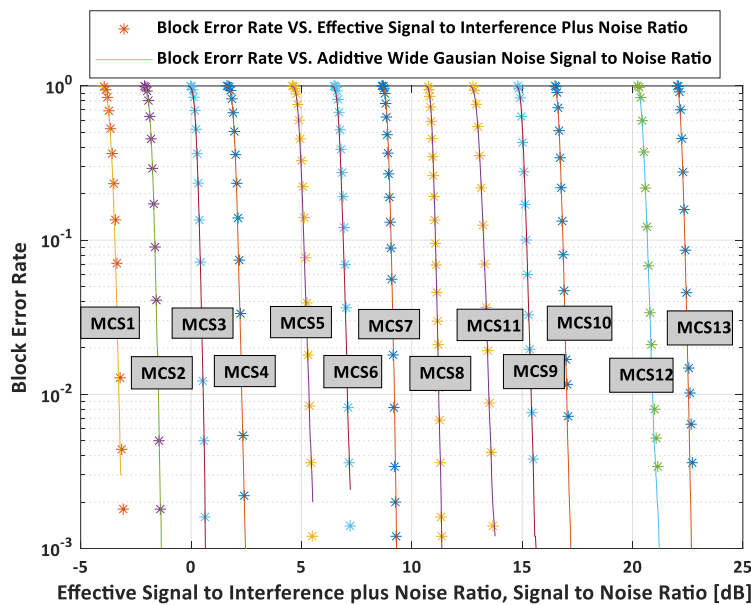


Fig. 4. Comparison between BLER curve with AWGN-SNR and BLER curve with ESINR.

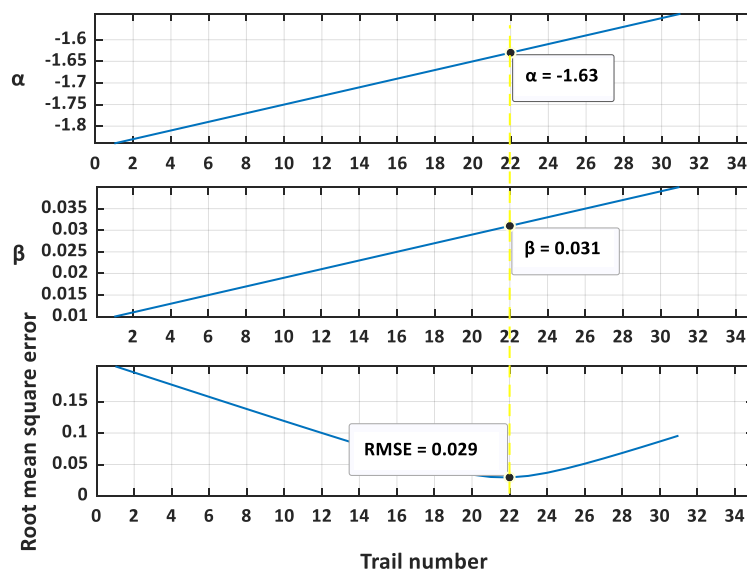


Fig. 5. Selection of optimum values of  $\alpha$  and  $\beta$  based on minimum RMSE (MCS2, RMS DS =30 ns).

Table 3. Optimized values of mapping function parameters for 30 ns RMS DS channel model.

MCS	1	2	3	4	5	6	7	8	9	10	11	12	13
$\alpha$	-3.37	-1.63	0.32	1.98	4.85	6.62	8.76	10.75	14.76	16.45	12.74	20.1	21.92
$\beta$	0.036	0.031	0.025	0.028	0.03	0.023	0.017	0.016	0.018	0.015	0.025	0.02	0.015
RMSE	0.038	0.029	0.038	0.031	0.041	0.037	0.032	0.023	0.019	0.03	0.042	0.047	0.065

Fig. 6 shows the BLER versus SNR performance of the PDSCH of the NR system using the LLS simulator (solid lines) and the proposed EESM abstraction model (markers plots) for the same SNR range considering AWGN and frequency selective channel with RMS DS of 30 ns. It is clear from the figure that the performance estimated using the proposed EESM model is close to the LLS model. Note that Fig. 6 shows the performance of a number of MCS modes for clarity.

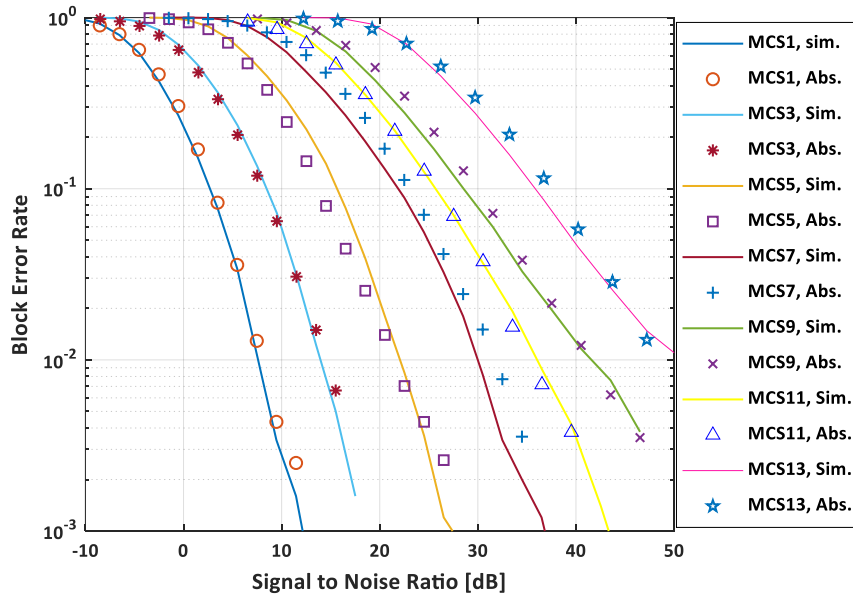


Fig. 6. Full simulation and abstract engine results.

As mentioned earlier, the aim of physical layer abstraction modelling is to minimize the simulation run time especially for system level studies. Performing system level studies using detail LLS of the physical layer is time consuming and not applicable for system level studies. Fig. 7 compares between simulation run time of the proposed EESM abstracted model and the detail LLS model of the PDSCH.

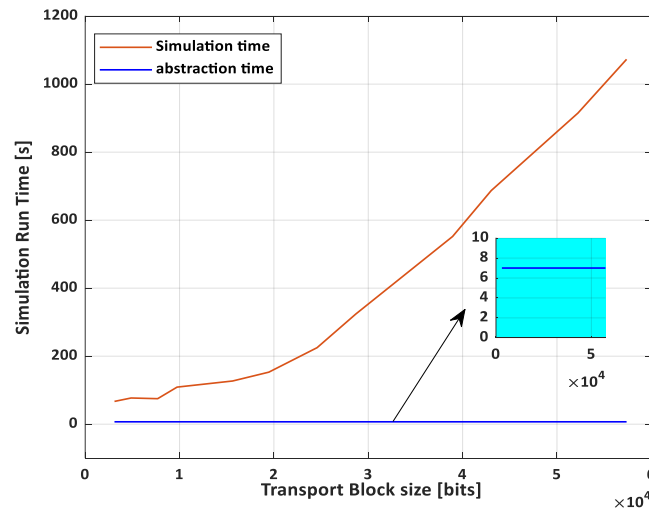


Fig. 7. Comparison between simulation and abstraction model run time.



The simulation of both models is performed on the same computing platform using a personal computer with processor (Intel core i7, 11<sup>th</sup> Generation, 11800H, 2.3 GHz). The comparison is performed for only one SNR point. The figure illustrates that the run time of the detailed LLS is significantly higher than the run time of the abstraction model. Furthermore, the run time of the detailed LLS increases when the size of transport block increases, but the run time of the abstract engine is constant and independent on the size of the transport block data.

#### 4. PROPOSED DELAY SPREAD BASED ABSTRACTION MODEL

The fitting of the ESINR mapping function parameters ( $\alpha$  and  $\beta$ ) in Eq. (1) alters when the channel realization changes [15]. Therefore, this section formulates novel equations for the dependency of the ESINR function on the RMS DS of the wireless channel. The RMS DS of a frequency selective wireless channel affects the performance of the wireless system. In other words, in addition to the MCS mode, the mapping function parameters ( $\alpha$  and  $\beta$ ) depend on the channel RMS DS. The proposed EESM abstraction model of Section 3 is used to evaluate the performance of a wireless system for different RMS DS in the range of 10 ns to 300 ns based on [21]. Optimum values for  $\alpha$  and  $\beta$  are selected for each RMS DS that provide minimum RMSE. The variation of  $\alpha$  and  $\beta$  versus the RMS DS of the channel are observed and formulated using *polyfit* function in MATLAB software.

Fig. 8 shows the variation of optimum values of  $\alpha$  and  $\beta$  versus RMS DS for different MCS modes. It is clear from Fig. 8 (a and b) that the optimum values of  $\alpha$  and  $\beta$  increase as the RMS delay spread increases. Therefore, it is necessary for accurate estimation of the wireless system performance to update the optimum values of  $\alpha$  and  $\beta$  in the EESM abstraction model based on the RMS DS of the link. For instance, Table 4 lists optimized values of  $\alpha$  and  $\beta$  for different RMS DSs considering MCS2. Also Fig. 9 shows graphs for the optimum values of  $\alpha$  and  $\beta$  versus RMS DS and their related fitted values for MCS 2. Fig. 9(a) illustrates  $\alpha$  curves, while Fig. 9(b) shows  $\beta$  curves. The blue curves of Fig. 9 are used to derive the related equations using *polyfit* feature in MATLAB software.

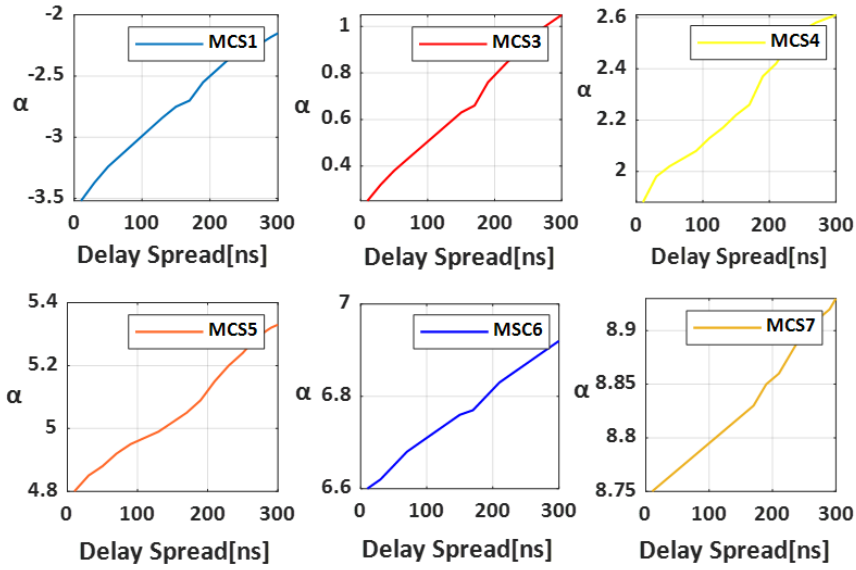
Table 4. Optimized values of  $\alpha$  and  $\beta$  in a range of examined DS for MCS2.

DS [ns]	$\alpha$	$\beta$	DS [ns]	$\alpha$	$\beta$
10	-1.75	0.023	170	-1.15	0.057
30	-1.64	0.030	190	-1.03	0.058
50	-1.55	0.035	210	-0.97	0.060
70	-1.46	0.040	230	-0.90	0.061
90	-1.40	0.044	250	-0.88	0.062
110	-1.32	0.050	270	-0.85	0.063
130	-1.25	0.053	290	-0.82	0.064
150	-1.18	0.055	300	-0.80	0.065

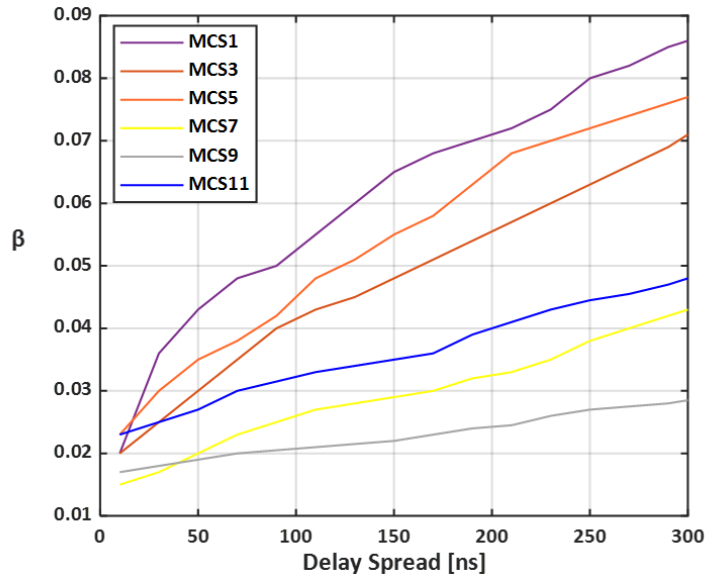
In general, both  $\alpha$  and  $\beta$  can be modelled using the second order equations in Eq. (4) and Eq. (5), respectively, in terms of coefficients  $a_0, a_1, a_2, b_0, b_1, b_2$ , and the RMS DS,  $S$ , in ns.

$$\alpha(S) = a_0 + a_1S + a_2S^2 \quad (4)$$

$$\beta(S) = b_0 + b_1S + b_2S^2 \quad (5)$$

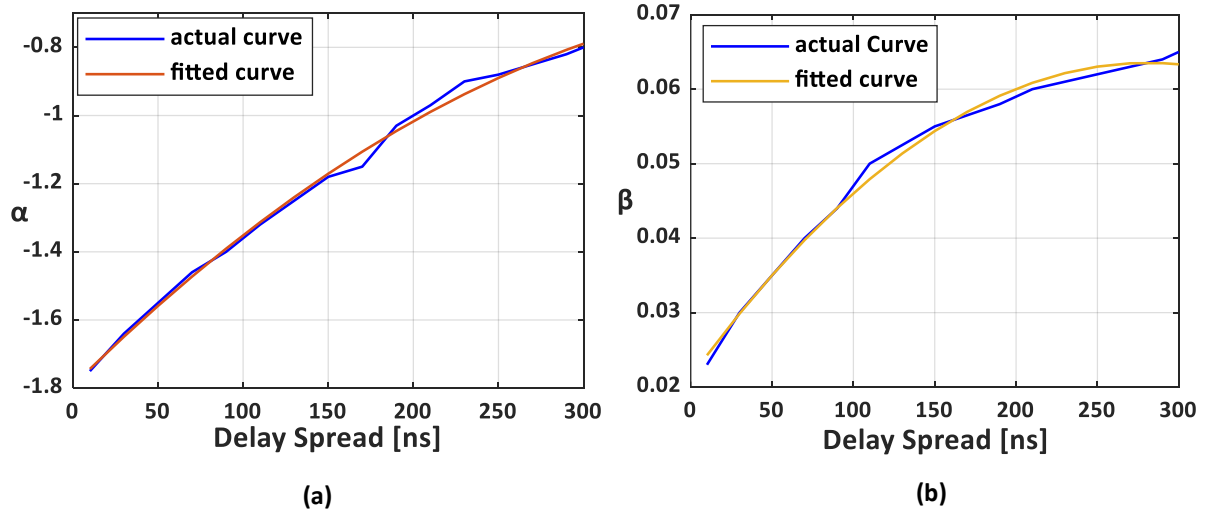


(a)



(b)

Fig. 8. Actual curves of ESINR mapping parameters versus RMS DS for different MCS modes: a)  $\alpha$  curves; b)  $\beta$  curves.



(a)

(b)

Fig. 9. Curves of ESINR mapping function parameters and their fitting for MCS mode 2: a)  $\alpha$  curves; b)  $\beta$  curves.

Table 5 lists the obtained coefficients of Eq. (4) and Eq. (5) that are required to calculate the optimum ESINR mapping parameters  $\alpha$  and  $\beta$  as a function of the RMS DS of the wireless channel,  $S$  (in ns) for different MCS modes considered in this study. It can be noticed from the table that these proposed equations are accurate because the RMSE values are small. These equations can be used to calculate  $\alpha$  and  $\beta$  and then the ESINR function of Eq. (1) based on the RMS DS of the channel. This provides accurate estimation of the NR wireless system in addition to reduced run time. Table 5 shows that the order of the equations of the EESM mapping parameters versus delay spread decreases from second order equations to first order and then to a constant as the MCS mode increases. The table also shows that the dependency of  $\alpha$  on the RMS DS decreases as the MCS mode increases. The mapping function  $\alpha$  starts to be constant for MCS 8 and above.

Table 5. Fitting coefficients and RMSE of  $\alpha$  and  $\beta$  for different MCS modes.

MCS Mode	Coefficients of $\alpha$				Coefficients of $\beta$			
	$a_0$	$a_1$	$a_2$	RMSE	$b_0$	$b_1$	$b_2$	RMSE
1	-3.6	0.006	$-5.1 \times 10^{-6}$	0.020	0.020	$3.4 \times 10^{-4}$	$-4.5 \times 10^{-7}$	0.002
2	-1.8	0.005	$-5.3 \times 10^{-6}$	0.010	0.020	$3 \times 10^{-3}$	$-5.3 \times 10^{-7}$	0.001
3	-0.2	0.003	0	0.010	0.020	$2.2 \times 10^{-4}$	$-1.8 \times 10^{-7}$	0.001
4	-1.9	0.003	0	0.020	0.020	$2.5 \times 10^{-4}$	$-2.5 \times 10^{-7}$	0.001
5	-4.8	0.002	0	0.020	0.020	$2.7 \times 10^{-4}$	$-2.8 \times 10^{-7}$	0.001
6	-6.6	0.001	0	0.005	0.020	$1.2 \times 10^{-4}$	0	$3 \times 10^{-4}$
7	8.7	$6.281 \times 10^{-4}$	0	0.006	0.015	$9 \times 10^{-5}$	0	0.001
8	10.8	0	0	-	0.014	$6.7 \times 10^{-5}$	0	$4 \times 10^{-4}$
9	14.8	0	0	-	0.017	$3.9 \times 10^{-5}$	0	$3 \times 10^{-4}$
10	16.5	0	0	-	0.014	$2.788 \times 10^{-5}$	0	$9 \times 10^{-4}$
11	12.7	0	0	-	0.020	$8.4 \times 10^{-5}$	0	$7 \times 10^{-4}$
12	20.1	0	0	-	0.020	0	0	-
13	21.9	0	0	-	0.015	0	0	-

## 5. CONCLUSIONS

This paper proposed a novel RMS delay spread based Exponential ESINR (EESM) abstraction model for the PDSCH of the 5G NR wireless system. A novel EESM formula with two tunable parameters is proposed for computing ESINR. The proposed model is validated using a detailed link level simulator of the PDSCH of the 5G NR system. Furthermore, models are proposed for different MCS modes to calculate optimum values for ESINR mapping parameters as a function of the RMS delay spread of the wireless channel. The channel is modelled using the TDL-A channel model.

The obtained results showed that the performance of the proposed abstraction model is very close to the performance of the link level simulation. The run time of the abstraction model is independent of the size of the transport block data. The abstraction model is 10 times faster than the detailed LLS for a transport block size of 3.1 kbits, while the factor increases to 153 times faster when the size of the transport block is increased to 57.376 kbits size.

The main contributions of the paper are proposing accurate EESM formula, and increasing the availability of the abstraction model through formulating the mapping function parameters with respect of channel model chaoticities.

The proposed model can be improved in the future studies by considering advanced optimization method for optimizing the mapping function parameters in order to speed up the optimization process. Also, the effect of changing the channel coding algorithms (the LDPC selected in this study) can be investigated in future studies.

## REFERENCES

- [1] O. Elalaouy, M. El-Ghzaoui, J. Foshi, "A low profile four-port MIMO array antenna with defected ground structure for 5G IoT applications," *Jordan Journal of Electrical Engineering*, vol. 9, no. 4, pp. 496-508, 2023, doi: 10.5455/jjee.204-1673904693.
- [2] N. Saadallah, S. Alabady, "A comprehensive study on energy efficient-cluster based routing protocols in the internet of things: hierarchical routing protocol," *Jordan Journal of Electrical Engineering*, vol. 9, no. 3, pp. 2409-9619, 2023, doi: 10.5455/jjee.204-1670351192.
- [3] S. Henry, A. Alshaily, E. Sousa, "5G is real: evaluating the compliance of the 3GPP 5G new radio system with the ITU IMT-2020 requirements," *IEEE Access*, vol. 8, no. 1, pp. 42828-42840, 2020, doi: 10.1109/ACCESS.2020.2977406.
- [4] K. Min, T. Kim, "Performance analysis on eigenmode beamforming for reduced capability device in massive MIMO systems," *IEEE Access*, vol. 11, no. 1, pp. 13103-13112, 2023, doi: 10.1109/ACCESS.2023.3242865.
- [5] M. Fuentes, J. Carcel, C. Dietrich, L. Yu, E. Garro, V. Pauli, F. Lazarakis, "5G new radio evaluation against IMT-2020 key performance indicators," *IEEE Access*, vol. 8, no. 1, pp. 110880-110896, 2020, doi: 10.1109/ACCESS.2020.3001641.
- [6] V. Garg, *An Overview of Digital Communication and Transmission, in Wireless Communications & Networking*, V. K. Garg Ed. Burlington: Morgan Kaufmann, 2007.
- [7] A. Omri, M. Shaqfeh, A. Ali, H. Alnuweiri, "Synchronization procedure in 5G NR systems," *IEEE Access*, vol. 7, no. 1, pp. 41286-41295, 2019, doi: 10.1109/ACCESS.2019.2907970.
- [8] 3GPP TS 38.212, 5G, 2020, [https://www.etsi.org/deliver/etsi\\_ts/138200\\_138299/138212/16.02.00\\_60/ts\\_138212v160200p.pdf](https://www.etsi.org/deliver/etsi_ts/138200_138299/138212/16.02.00_60/ts_138212v160200p.pdf).
- [9] 3GPP TS 38.211, 5G, 2020, [https://www.etsi.org/deliver/etsi\\_ts/138200\\_138299/138211/16.02.00\\_60/ts\\_138211v160200p.pdf](https://www.etsi.org/deliver/etsi_ts/138200_138299/138211/16.02.00_60/ts_138211v160200p.pdf)
- [10] S. Lagen, K. Wanuga, H. Elkotby, S. Goyal, N. Patriciello, L. Giupponi, "New radio physical layer abstraction for system-level simulations of 5G networks," *IEEE International Conference on Communications*, 2020, doi: 10.1109/ICC40277.2020.9149444.
- [11] C. Li, C. Wenwen, W. Bin, Z. Xin, C. Hongyang, Y. Dacheng, "System-level simulation methodology and platform for mobile cellular systems," *IEEE Communications Magazine*, vol. 49, no. 7, pp. 148-155, 2011, doi: 10.1109/MCOM.2011.5936168.
- [12] M. Müller, F. Ademaj, T. Dittrich, A. Fastenbauer, B. Elbal, A. Nabavi, L. Nagel, S. Schwarz, M. Rupp, "Flexible multi-node simulation of cellular mobile communications: the Vienna 5G System Level Simulator," *EURASIP Journal on Wireless Communications and Networking*, vol. 2018, no. 1, p. 227, 2018, doi: 10.1186/s13638-018-1238-7
- [13] W. Anwar, K. Kulkarni, T. Augustin, N. Franchi, G. Fettweis, "PHY abstraction techniques for IEEE 802.11p and LTE-V2V: applications and analysis," *IEEE Globecom Workshops*, 2018, doi: 10.1109/GLOCOMW.2018.8644470.
- [14] W. Anwar, S. Dev, K. Kulkarni, N. Franchi, G. Fettweis, "On PHY Abstraction modeling for IEEE 802.11ax based multi-connectivity networks," *IEEE Wireless Communications and Networking Conference*, 2019, doi: 10.1109/WCNC.2019.8885654.

- [15] E. Chu, J. Yoon, B. Jung, "A novel link-to-system mapping technique based on machine learning for 5G/IoT wireless networks," *Sensors*, vol. 19, no. 5, p. 1196, 2019, doi: 10.3390/s19051196.
- [16] W. Anwar, A. Kumar, N. Franchi, G. Fettweis, "Performance analysis using physical layer abstraction modeling for 5G and beyond waveforms," *IEEE Global Communications Conference*, 2019, doi: 10.1109/GLOBECOM38437.2019.9014130.
- [17] W. Anwar, K. Kulkarni, N. Franchi, G. Fettweis, "Physical layer abstraction for ultra-reliable communications in 5G multi-connectivity networks," *IEEE 29th Annual International Symposium on Personal, Indoor and Mobile Radio Communications*, 2018, doi: 10.1109/PIMRC.2018.8580956.
- [18] 3GPP TS 38.214, 5G, 2020, [https://www.etsi.org/deliver/etsi\\_ts/138200\\_138299/138214/16.02.00\\_60/ts\\_138214v160200p.pdf](https://www.etsi.org/deliver/etsi_ts/138200_138299/138214/16.02.00_60/ts_138214v160200p.pdf).
- [19] S. Ahmadi, *New Radio Access Physical Layer Aspects (Part 2) in 5G NR*, S. Ahmadi Ed.: Academic Press, 2019.
- [20] 3GPP TS 38.104, 5G, 2020, [https://www.etsi.org/deliver/etsi\\_ts/138100\\_138199/138104/16.04.00\\_60/ts\\_138104v160400p.pdf](https://www.etsi.org/deliver/etsi_ts/138100_138199/138104/16.04.00_60/ts_138104v160400p.pdf).
- [21] 3GPP TR 38.901, 5G, 2020, [https://www.etsi.org/deliver/etsi\\_tr/138900\\_138999/138901/16.01.00\\_60/tr\\_138901v160100p.pdf](https://www.etsi.org/deliver/etsi_tr/138900_138999/138901/16.01.00_60/tr_138901v160100p.pdf).